Antonie van Leeuwenhoek (2026) 119:146
https://doi.org/10.1007/s10482-026-02356-0

ORIGINAL PAPER

Cellulomonas electrica sp. nov., isolated from an electrochemical enrichment culture

Sota Ihara · Akihiro Okamoto

Received: 20 August 2025 / Accepted: 5 June 2026

Abstract A Gram-positive, facultatively anaerobic, rod-shaped actinomycete bacterium, strain NTE-D12^T was isolated from the filtrate (< 0.22 µm pore size) of an electrochemical enrichment culture. The strain grew in R2A medium at 15–40 °C (optimum 30 °C), pH 6–8 (optimum pH 6), and in the presence of 0–6% NaCl (optimum 0%). Phylogenetic analysis based on 16S rRNA gene sequences showed that strain NTE-D12^T is closely related to *Cellulomonas algicola* TKZ-21^T (97.9%), *Cellulomonas biazotea* DSM 20112^T (97.5%), and *Cellulomonas fimi* DSM 20113^T (97.5%). Genome-based phylogenetic analysis indicated that the closest relative is *Cellulomonas citrea* AO-9^T. Orthologous average nucleotide identity (OrthoANI) and digital DNA–DNA hybridization (dDDH) values between strain NTE-D12^T and related species ranged from 75.40–76.73% and 20.2–21.0%, respectively, clearly below the species delineation thresholds. In contrast, average amino acid identity (AAI) and percentage of conserved proteins (POCP) values ranged from 68.33–70.89% and 58.33–62.26%, respectively, indicating affiliation within the genus *Cellulomonas*. The major polar lipids were diphosphatidylglycerol, phosphatidylinositol, aminoglycophospholipid, and glycophospholipid. The peptidoglycan type was A4β with L-Orn–D-Ser–D-Glu. The predominant cellular fatty acid was anteiso-$C_{15:0}$ (65.6%). The major quinone was menaquinone-10, distinguishing the strain from the other *Cellulomonas* species. The genomic DNA GC content was 73.1%. Based on phenotypic, phylogenetic, and chemotaxonomic characteristics, strain NTE-D12^T (= NBRC

Supplementary Information The online version contains supplementary material available at https://doi.org/10.1007/s10482-026-02356-0.

S. Ihara
Graduate School of Science and Technology, University of Tsukuba, 1-1-1 Tennodai, Tsukuba 305-8572, Japan

S. Ihara · A. Okamoto (✉)
International Center for Materials Nanoarchitectonics (WPI-MANA), National Institute for Materials Science (NIMS), 1-1 Namiki, Tsukuba 305-0044, Japan
e-mail: OKAMOTO.Akihiro@nims.go.jp

S. Ihara · A. Okamoto
Research Center for Macromolecules and Biomaterials, National Institute for Materials Science (NIMS), 1-1 Namiki, Tsukuba 305-0044, Japan

A. Okamoto
Graduate School of Chemical Sciences and Engineering, Hokkaido University, North 13 West 8, Kita-ku, Sapporo 060-8628, Japan

A. Okamoto
Graduate School of Life and Environmental Sciences, University of Tsukuba, 1-1-1 Tennodai, Tsukuba 305-8577, Japan

A. Okamoto
Research Center for Autonomous Systems Materialogy (ASMat), Institute of Integrated Research (IIR), Institute of Science Tokyo (Science Tokyo), 4259 Nagatsuta-cho, Midori-ku, Yokohama, Kanagawa 226-8503, Japan

Published online: 12 June 2026

115591^T = DSM 114595^T) represents a novel species of the genus *Cellulomonas*, for which the name *Cellulomonas electrica* sp. nov. is proposed.

Keywords *Cellulomonas* · Extracellular electron transfer · 0.22 µm filtrate · Average nucleotide identity analysis · Major quinone profile

Abbreviations

EET	Extracellular electron transfer
orthoANI	Orthologous average nucleotide identity
dDDH	Digital DNA–DNA hybridization
AAI	Average amino acid identity
POCP	Percentage of conserved proteins
PCR	Polymerase chain reaction
BLASTN	Nucleotide basic local alignment search tool
MUSCLE	Multiple sequence comparison by log-expectation
NJ	Neighbor-joining
MP	Maximum-parsimony
ML	Maximum-likelihood
GTDB	Genome Taxonomy Database
SEM	Scanning electron microscopy
TEM	Transmission electron microscopy
FAMES	Fatty acid methyl esters
ENIU	Equivalent number of isoprene units
MK	Menaquinone
DPG	Diphosphatidylglycerol
PI	Phosphatidylinositol
AGPL	Aminoglycophospholipid
GPL	Glycophospholipid
Ala	Alanine
Glu	Glutamic acid
Ser	Serine
Orn	Ornithine

Introduction

Extracellular electron transfer (EET) is a respiratory system that facilitates direct electron transfer to conductive solids (Myers and Nealson 1988; Shi et al. 2016). While the core mechanisms and vital genes associated with EET have been detailed in Gram-negative bacteria, primarily focusing on the genera *Shewanella* and *Geobacter* (Lovley and Phillips 1988; Myers and Nealson 1988), a myriad of other bacteria exhibit EET capabilities, even in Gram-positive bacteria (Wrighton et al. 2011; Naradasu et al. 2019, 2020; Pankratova et al. 2019). Light et al. elucidated this mechanism specifically in *Listeria monocytogenes* (Light et al. 2018). Nevertheless, the number of Gram-positive bacteria identified with EET abilities pales in comparison to Gram-negative species. Thus, our understanding of EET mechanisms in gram-positive bacteria, beyond *L. monocytogenes*, remains limited. Uncovering novel Gram-positive EET-capable bacteria is vital to broadening our understanding of their underlying mechanisms.

The genus *Cellulomonas*, classified under the family Cellulomonadaceae and first described in 1923, comprises Gram-positive, aerobic bacteria (Bergey et al. 1923). Forty-one species have been recognized and isolated from diverse environments, such as termite gut, deep-sea and terrestrial environments (Zhang et al. 2013; Sun et al. 2018; Lee et al. 2020). Recent findings spotlight certain *Cellulomonas* ability to employ cellulose or glucose as electron donors and carbon electrodes as ultimate electron acceptors, hinting at their potential application in microbial fuel cells (Khawdas et al. 2019).

Cellulomonas sp. strain NTE-D12^T was isolated from an electrochemical enrichment of a soil-derived sample that had been passed through a 0.22 µm filter (Ihara et al. 2022). Intriguingly, the majority of microorganisms that pass through the 0.22 µm filter exhibit phylogenetic diversity (Naganuma et al. 2007; Nakai et al. 2013). In particular, the strain NTE-D12^T showcases an elevated current production capability and houses a distinct electron carrier activity gene cluster, setting it apart from related species in terms of its enhanced EET proficiency (Ihara et al. 2022).

Our study embarked on a comprehensive analysis of the phenotype, chemotaxonomy, and molecular phylogeny of strain NTE-D12^T. Our findings reveal several distinguishing traits compared to the relative strains. Notably, the Orthologous average nucleotide identity (orthoANI) and digital DNA–DNA hybridization (dDDH) analyses solidified the unique classification of NTE-D12^T. Consequently, we suggest that strain NTE-D12^T be recognized as a novel species within the genus *Cellulomonas*, for which the name *Cellulomonas electrica* sp. nov. is proposed.

Materials and methods

Molecular analysis

The Quick-DNA HMW MagBead Kit (Zymo Research, Irvine, CA, USA) was used for genomic DNA extraction. We used universal primers, 27F (5′-AGAGT TTGAT CCTGG CTCAG -3′) and 1492R (5′- GGTTA CCTTG TTACG ACTT-3′), to amplify the near full-length of 16S rRNA gene by polymerase chain reaction (PCR). The PCR product was purified using the NucleoSpin® Gel and PCR Clean-up (Takara Bio, Kusatsu, Shiga, Japan). The amplified PCR products were directly sequenced. To construct the nearly full-length 16S rRNA gene, the obtained sequence data were compiled using BioEdit software (Hall 1999). The nearly full-length 16S rRNA gene (1,403 bp) was compared to existing sequences in the national center for biotechnology information rRNA/ITS database using the nucleotide basic local alignment search tool (BLASTN) program (Altschul et al. 1990).

Whole genome sequence, de novo assembly, and gene annotation were conducted in the previous study (accession no. AP026442) (Ihara et al. 2022). The genome completeness was evaluated using CheckM2 ver 1.0.2 (Chklovski et al. 2023). OrthoANI and dDDH values were compared between related species using EzBio Cloud server (Lee et al. 2016) and Genome-to-Genome Distance Calculator 3.0 (Auch et al. 2010), respectively. Average amino acid identity (AAI) and the percentage of conserved proteins (POCP) were calculated using CompareM v0.1.2 (https://github.com/dparks1134/CompareM) and the Nextflow-based POCP-nf pipeline (https://github.com/hoelzer/pocp) to assess genus-level novelty.

Sequence data of 16S rRNA genes and whole genomes of related type strains were retrieved from the GenBank database. For 16S rRNA gene analysis, sequences were aligned using the MUSCLE program (Edgar 2004). The alignment was trimmed to positions 83–1427 according to the *Escherichia coli* numbering system (Brosius et al. 1978). Phylogenetic trees based on 16S rRNA gene sequences were constructed using the neighbor-joining (NJ) (Saitou and Nei 1987) and maximum-likelihood (ML) (Felsenstein 1981) methods with the Jukes–Cantor substitution model and maximum-parsimony (MP) (Takahashi and Nei 2000) method with the Subtree-Pruning-Regrafting algorithm implemented in the MEGA11 program (Tamura et al. 2021). Tree topologies were evaluated by bootstrap analysis with 1,000 resamplings (Felsenstein 1985). For genome-based phylogenetic analysis, single-copy housekeeping genes were identified and aligned using GTDB-Tk v2.4.0 with the Bac120 marker set. The resulting alignments were trimmed using trimAl v1.5.0 with the automated trimming option (Capella-Gutierrez et al. 2009). A maximum-likelihood phylogenetic tree was then constructed using IQ-TREE2 v2.3.6 with the LG + F + G4 substitution model. Branch support was assessed using 1,000 ultrafast bootstrap replicates and 1,000 SH-like approximate likelihood ratio tests (Minh et al. 2020).

Physiological analysis

R2A medium was used to determine the growth ranges for temperature, pH, and NaCl concentration. Growth at different temperatures was assessed by incubating strain NTE-D12^T on R2A agar plates at 4, 10, 15, 20, 30, 37, 40, and 45 °C for 14 days. The pH range for growth was determined in buffered R2A liquid medium at 30 °C over a pH range of 4.0–10.0 for 14 days. The medium was buffered as follows: pH 4.0–5.0 with 0.1 M citric acid/0.1 M sodium citrate; pH 6.0–8.0 with 0.1 M KH_2PO_4/0.1 M NaOH; and pH 9.0–10.0 with 0.1 M $NaHCO_3$/0.1 M Na_2CO_3. Growth at different NaCl concentrations (0–7%, w/v) was examined in R2A liquid medium at 30 °C for 14 days. All cultures were incubated aerobically with shaking at 180 rpm. Anaerobic growth was tested in Gifu anaerobic medium after purging with N_2/CO_2 (80:20, v/v) gas for 1 h, followed by incubation for 5 days. All growth experiments were performed in triplicate. Enzymatic activities and carbon source utilization were evaluated using API ZYM and API 50CHL systems (bioMérieux, Marcy-l'Étoile, France), according to the manufacturer's instructions. Cellulose degradation was assessed using CMC-Na agar [composition (g L^{-1}): 5.0 CMC-Na, 1.0 KNO_3, 0.5 $MgSO_4{\cdot}5H_2O$, 0.01 $FeSO_4{\cdot}7H_2O$, 1.0 tryptone, and 15.0 agar]. Bacterial suspensions ($OD_{600} = 0.5$, 10 µL) were spotted onto the plates and incubated at 30 °C for 7 days. Plates were then stained with 0.1% (w/v) Congo red solution for 20 min and destained with 1 M NaCl, followed by three washes. Cellulose degradation was evaluated based on the formation of clear zones (Sun et al. 2018).

Electrochemical measurements of strain NTE-D12^T were performed using a single-chamber three-electrode system as described previously (Naradasu et al. 2019), with a tin-doped indium oxide (ITO) glass working electrode, a platinum wire counter electrode, and an Ag/AgCl (sat. KCl) reference electrode. The electrolyte consisted of 4.0 mL defined medium (DM) [composition (g L^{-1}): 1.0 NH_4Cl, 0.8 $MgCl_2{\cdot}6H_2O$, 0.1 $CaCl_2{\cdot}2H_2O$, 0.5 KH_2PO_4, and 1.0 $NaHCO_3$]. Cells were cultured in R2A liquid medium for 30 h, harvested, washed twice with DM, and resuspended in DM to an OD_{600} of 5.0, followed by purging with > 99.9% N_2 gas for 30 min. During the electrochemical measurements, a 0.5 mL aliquot of the cell suspension and 0.5 mL of either glucose solution (100 g L^{-1}) or sterile water were added to the reactor, resulting in a final OD_{600} of 0.5 and a final glucose concentration of 10 g L^{-1} (when added). Electrochemical measurements were performed by single-potential amperometry using an automatic polarization system (VMP3; Bio-Logic Science Instruments) at 30 °C, with the working electrode poised at + 0.2 V (vs. Ag/AgCl, sat. KCl).

Morphological characterization

Single colonies were obtained on R2A agar after incubation at 30 °C for 24 h. Colony morphology was examined after cultivation on R2A agar for 14 days at 30 °C. Gram staining was performed as described in Hucker method (Gerhardt et al. 1981). Cell morphology was observed using scanning electron microscopy (SEM) and transmission electron microscopy (TEM) after aerobic cultivation in R2A medium for 30 h. SEM observations were carried out following previously described procedures(Ihara et al. 2022). The cells were stained with 2% phosphotungstic acid for TEM observation. TEM observation was outsourced to Tokai Electron Microscopy, Inc (Aichi, Japan).

Chemotaxonomic characterization

Cells for fatty acid analysis were grown aerobically at 28 °C for 4 days. Wet biomass was collected by centrifuge at 7,000 g and converted to fatty acid methyl esters (FAMEs) using a methylation kit (Nacalai Tesque, Japan). FAMEs were analyzed by GC/MS (8890 GC coupled with MSD 5977B; Agilent Technologies) using an HP-88 column (30 m × 0.25 mm, 0.20 µm) with helium as the carrier gas and an injector temperature of 250 °C. The oven temperature was programmed from 80 °C (2 min) to 130 °C at 10 °C min^{-1} (15 min hold), then to 160 °C at 3 °C min^{-1}, and finally to 200 °C at 20 °C min^{-1} (6 min hold). Detection was performed in scan mode, and fatty acids were identified based on retention times and mass spectra using FAME standards (Cayman Chemical). Cells for other chemotaxonomic analyses were grown aerobically at 30 °C for 30 h. Total lipids were extracted using the revised Bligh and Dyer method (Bligh 1959), and quinones were purified by solid-phase extraction (Sep-Pak Plus silica; Waters). Quinone profiles were analyzed using an ACQUITY UPLC H-Class system (Waters) equipped with a BEH C18 column (2.1 × 150 mm, 1.7 µm) under the following conditions: methanol/isopropanol (7:3, v/v) as the mobile phase, flow rate 0.3 mL min^{-1}, and column temperature 35 °C. Quinones were identified using authentic standards or estimated based on the equivalent number of isoprene units (ENIU) (Tamaoka et al. 1983). Polar lipids were analyzed by two-dimensional thin-layer chromatography with appropriate detection reagents (Minnikin et al. 1977; Yassin et al. 1993). Peptidoglycan was hydrolyzed with 4 N HCl at 100 °C for 4 h and analyzed by GC/MS as N-heptafluorobutyric acid isobutyl esters (Schumann 2011; Schumann et al. 2021).

Fatty acid analysis was performed by Dojin-Glocal Co., Ltd. (Kumamoto, Japan), quinone analysis by Techno Suruga Lab Co., Ltd. (Shizuoka, Japan), and polar lipid and peptidoglycan analyses by DSMZ Services (Braunschweig, Germany).

Results and discussion

16S rRNA gene and genome-based phylogenetic analysis

A nearly full-length 16S rRNA gene sequence (1,403 bp) was obtained. Based on the maximum-likelihood (ML) phylogenetic tree, strain NTE-D12^T clustered within the genus *Cellulomonas* (Fig. 1). The three closest relatives were *Cellulomonas algicola* TKZ-21^T, *Cellulomonas biazotea* DSM 20112^T and *Cellulomonas fimi* 20113^T, showing 16S rRNA gene sequence similarities of 97.9%,

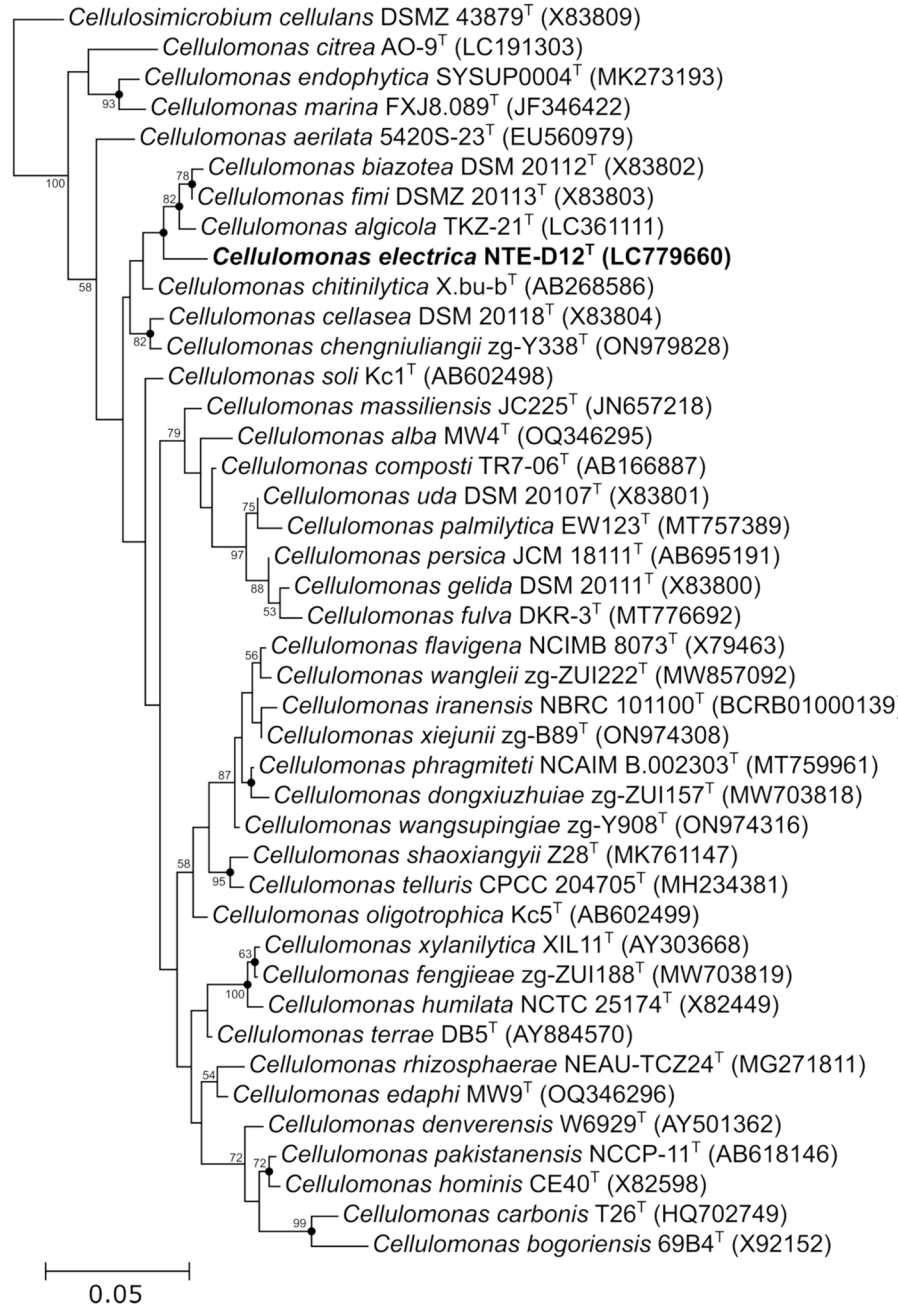

Fig. 1 Phylogenetic tree derived from 16S rRNA gene sequences between strain NTE-D12^T and the type strains of related *Cellulomonas* species. The tree was constructed using the Maximum-likelihood method using the Jukes-Cantor model. The black circular dot indicates that corresponding nodes were also recovered in trees generated with the maximum-parsimony method using the Subtree-Pruning-Regrafting algorithm and neighbor-joining method using the Jukes-Cantor model. Numbers at branch points indicate bootstrap percentages (only values ≥ 50% are shown). Bar, 0.01 nucleotide substitution position

97.5%, and 97.5%, respectively. The neighbor-joining (NJ) and maximum-parsimony (MP) trees also supported these three species as the closest relatives (Figs. S1 and S2). However, the bootstrap support for the clustering between strain NTE-D12^T and *C. algicola* was below 50% in these 16S rRNA gene trees, indicating low confidence in this relationship. In contrast, genome-based phylogenomic analysis identified *Cellulomonas citrea* Ao-9^T as the closest relative (Fig. 2). The phylogenomic tree was strongly supported, with ultrafast bootstrap and SH-aLRT values of 96.7% and 97%, respectively, indicating high reliability. Compared with the 16S rRNA gene-based phylogeny, the genome-based phylogeny provided a more robust inference of the evolutionary relationship.

Genome-based species and genus delineation

The complete genome of strain NTE-D12^T consists of one circular chromosome (3.68 Mbp) and one circular plasmid (5,386 bp) with 99.97% completeness evaluated using CheckM2. The whole genome contains 6 rRNA, 54 tRNA, 1 tmRNA and 3,333 CDSs. The genome has 73.1% G + C content.

OrthoANI and dDDH values between strain NTE-D12^T and its related type strains were less than 76.63% and 21.0%, respectively (Table 1). These values are well below the accepted species delineation thresholds of 95–96% for OrthoANI and 70% for dDDH (Rosselló-Mora and Amann 2001; Goris et al. 2007). In contrast, AAI and POCP values between strain NTE-D12^T and related type strains were below 70.89% and 62.26%, respectively. These values fall within or above the proposed genus-level thresholds (AAI: 65–72%; POCP: 50%) (Qin et al. 2014; Konstantinidis et al. 2017). Collectively, these results indicate that strain NTE-D12^T represents a novel species but does not constitute a novel genus.

Physiological and morphological features

Growth of strain NTE-D12^T occurred at 20–40 °C, at pH 6–7, and in the presence of 0–2% NaCl for 7 days of incubation. Growth was also observed at 15 °C, pH 8, and 3–6% NaCl after 14 days. In summary, this strain grew at 15–40 °C, pH 6–8, and in the presence of 0–6% NaCl. Strain NTE-D12^T was able to utilize D-arabinose, which is not utilized by most related species, whereas it did not utilize amygdalin, which is utilized by most related species (Table 2). The cellulose degradation activity was weaker than that of related species (Fig. S3). Colonies grown on R2A agar plate were circular, undulating, and lemon-yellow in color (Fig. S4). During electrochemical measurements, strain NTE-D12^T exhibited a gradual increase in current upon glucose addition compared to the no-glucose control, reaching a maximum of 238 nA cm^{-2} at 112 h (Fig. S5). This indicates that the strain can generate current using glucose as an electron donor.

Cells observed to be Gram-positive using optical microscopy. Rod shaped, flagellated cells were observed using TEM, and the size was length × width = 0.9 to 1.8 × 0.4 to 0.6 µm (Fig. 3). As demonstrated in a previous study, isolated cells did not pass through a 0.22 µm filter again (Ihara et al. 2022). It is presumed that the NTE-D12^T may only attain a filter-passing size under specific conditions such as environmental stresses (Hood and MacDonell 1987).

Table 1 Genome comparison between strain NTE-D12^T and closely related *Cellulomonas* species

Taxon (Accession No.)	orthoANI value (%)	dDDH (d0; %)	dDDH (d4; %)	dDDH (d6; %)	AAI (%)	POCP (%)
Cellulomonas citrea AO-9^T (GCA_009829685.1)	76.19	19	20.2	18.4	70.39	62.26
Cellulomonas endophytica SYSUP0004^T (GCA_004123805.1)	75.40	15.9	20.5	16.9	68.33	59.07
Cellulomonas marina NBRC 110784^T (GCA_016862715.1)	75.52	17	20.5	15.9	69.07	60.20
Cellulomonas algicola TKZ-21^T (GCA_003851725.1)	76.73	17.7	21	17.5	70.68	58.33
Cellulomonas biazotea DSM 20112^T (GCF 004306155.1)	76.51	18.5	20.6	18.1	70.89	59.47
Cellulomonas fimi DSM 20113^T (GCA_000212695.1)	76.39	19.2	20.4	18.6	70.75	61.61

Values are presented as differences relative to strain NTE-D12^T. OrthoANI was calculated using the EZBioCloud server(https://www.ezbiocloud.net/tools/ani), and dDDH values were estimated using GGDC 3.0 (https://ggdc.dsmz.de/distcalc2.php). AAI was calculated using CompareM v0.1.2 (https://github.com/dparks1134/CompareM), and POCP was determined using the Nextflow-based POCP-nf pipeline (https://github.com/hoelzer/pocp)

Table 2 Differential characteristics between strain NTE-D12^T and closely phylogenetic relative species

Characteristics	1	2	3	4	5	6	7
Growth at:							
6% NaCl	+	−	−	−	−	−	−
pH 9.0	−	+	+	−	+	+	−
Cell size (length × width, μm)	0.9–1.8 × 0.4 − 0.6	2.0–2.4 × 0.5–0.8	N/A	N/A	0.5–0.8 × 0.4–0.5	N/A	N/A
Margin of colony	undulate	entire	N/A	N/A	curled	entire	entire
Major fatty acid* (> 10%)	anteiso-$C_{15:0}$	anteiso-$C_{15:0}$ C:$_{16:0}$ $C_{14:0}$	anteiso-$C_{15:0}$ anteiso-$C_{15:1}$ A C:$_{16:0}$	anteiso-$C_{15:0}$ C:$_{16:0}$	anteiso-$C_{15:0}$ iso-$C_{15:0}$	anteiso-$C_{15:0}$ iso-$C_{16:0}$ iso-$C_{15:0}$ iso-$C_{14:0}$	anteiso-$C_{15:0}$ C:$_{16:0}$ iso-$C_{16:0}$
Major menaquinone	MK-10	MK-9 (H_4)	MK-9 (H_4)	MK-9 (H_4)	MK-9 (H_4)	MK-9 (H_4)	MK-9 (H_4)
Carbon source utilization:							
D-Arabinose	+	−	N/A	−	−	−	−
L-Rhamnose	−	−	+	+	+	+	+
D-Mannitol	+	−	−	+	−	+	−
Methyl-α-D-glucopyranoside	−	+	N/A	N/A	+	−	−
Amygdalin	−	+	N/A	N/A	+	+	+
D-Melibiose	−	−	+	−	+	+	+
D-Melezitose	−	−	N/A	N/A	+	+	+
D-Raffinose	−	−	+	−	+	+	+
Enzymatic activities:							
Valine allyl amidase	+	−	+	N/A	−	−	−
Cystine allyl amidase	+	−	+	N/A	−	−	−
α-Galactosidase	+	−	+	N/A	−	−	−

Strain: 1, NTE-D12^T; 2, *C.citrea* AO-9^T; 3, *C.endophytica* SYSUP0004^T; 4, *C.marina* FXJ8.089^T; 5, *C.algicola* TKZ-21^T; 6, *C.biazotea* DSM 20112^T; 7, *C.fimi* DSM 20113^T

1: Data obtained from the present study, 2: Data referred from Lee et al. 2020 (Lee et al. 2020), 3: Data referred from Li et al. 2020 (Li et al. 2020), 4: Data referred from Zhang et al. 2013 (Zhang et al. 2013), 5,6,7: Data referred from Yamamura et al. 2019 (Yamamura et al. 2019), +, positive; w, weakly positive; −, negative; N/A, no data available

*Fatty acid profiles for strains 1, 2, and 5–7 were determined in this study; detailed data are provided in Table S1 (Supplementary file)

Chemotaxonomic characteristics

The cellular fatty acid profiles (> 1% of the total fatty acids) were anteiso-$C_{15:0}$ (65.6%), $C_{14:0}$ (9.4%), $C_{16:0}$ (8.7%), iso-$C_{16:0}$ (6.8%), iso-$C_{14:0}$ (5.7%), iso-$C_{15:0}$ (2.1%), and anteiso-$C_{17:0}$ (1.6%) (Table S1).

Most members of the genus *Cellulomonas* possess menaquinone (MK)-9(H_4) as the predominant quinone, although MK-8(H_4) has been reported in some species (Kang et al. 2007). However, the presence of MK-10 as the predominant quinone has not been reported in this genus. The major peak of strain NTE-D12^T appeared at 7.72 min, which is closer to the retention time of MK-10 standard (7.73 min) than to the estimated retention time of MK-9(H_4) (7.30 min) based on ENIU, and was therefore assigned to MK-10 (Fig. S6). Although the quinone composition deviates from typical *Cellulomonas* species, genome-based phylogenetic metrics (AAI, POCP, and phylogenomics) consistently support its placement within the genus, indicating that quinone

variation alone does not warrant genus-level reclassification. Taken together, these results indicate that strain NTE-D12^T is the first *Cellulomonas* species possessing MK-10 as the predominant quinone.

The major polar lipids consisted of diphosphatidylglycerol (DPG), phosphatidylinositol (PI), aminoglycophospholipid (AGPL), and glycophospholipid (GPL). Some unidentified phospholipids, aminolipids and lipids were observed as minor polar lipids (Fig. S7). The peptidoglycan contained the amino acids alanine (Ala), glutamic acid (Glu), serine (Ser), and ornithine (Orn) in the following molar ratio: 2.5: 2.0: 0.9: 0.4, respectively. The analysis of enantiomers showed the presence of D-Ser, L-Orn, D-Ala/L-Ala and D-Glu. Based on the obtained data, the peptidoglycan was classified as type A4β with L-Orn–D-Ser–D-Glu, which is the same peptidoglycan type as in related species.

Taxonomic conclusions

We characterized strain NTE-D12^T, isolated from an electrochemical enrichment culture of a 0.22 µm pore-size filter filtrate, based on phylogenetic, phenotypic, and chemotaxonomic analyses. Strain NTE-D12^T was clearly separated from related type strains of *Cellulomonas* in both the 16S rRNA gene-based phylogenetic tree and the GTDB-based phylogenomic tree (Figs. 1 and 2).

The ANI and dDDH values between strain NTE-D12^T and related species were below 76.73% and 21.0%, respectively. In addition, the AAI and POCP values were consistent with assignment to the genus *Cellulomonas*, indicating that strain NTE-D12^T does not represent a novel genus. The major quinone was MK-10, which differs from the predominant MK-9(H_4) observed in related species.

Based on the results of the phylogenetic, phenotypic, and chemotaxonomic characterizations, strain NTE-D12^T represents a novel species within the genus *Cellulomonas*, for which the name *Cellulomonas electrica* is proposed.

Description of *Cellulomonas electrica* sp. nov.

Cellulomonas electrica (e.lec'tri.ca. L. neut. n. electrum, amber; N.L. fem. adj. electrica, pertaining to electricity).

Cells are found to be Gram-stain positive, facultatively anaerobic, rod-shaped 0.9–1.8 µm long and 0.4–0.6 µm wide. Colonies formed on R2A agar are circular, undulate, and lemon-yellow color. Growth occurs at 15–40 °C (optimum 30 °C), pH 6–8 (optimum pH 6), and in 0–6% (w/v) NaCl (optimum 0%). Weakly positive for degradation of cellulose. With the API 50ch system, The following compounds are found to be capable of utilizing as a carbon source: glycerol, D-arabinose, L-arabinose, D-xylose, D-galactose, D-glucose, D-fructose, D-mannose, D-mannitol, N-acetyl-glucosamine, arbution, esculin ferric citrate, salicin, D-cellobiose, D-maltose, D-sucrose, D-trehalose, starch, glycogen, gentiobiose, D-turanose, and D-lyxose as a solo carbonsource, but are not found to be capable of utilizing Erythritol, D-ribose, L-xylose, D-adonitol, methyl-β-D-xylopyranoside, L-sorbose, L-rhamnose, dulcitol, inositol, D-sorbitol, methyl-α-D-mannopyranoside, methyl-α-D-Glucopyranoside, amygdalin, D-lactose, D-melibiose, Inulin, D-melezitose, D-raffinose, xylitol, D-tagatose, D-fucose, L-fucose, D-arabitol, L-arabitol, gluconate, 2-keto-gluconate, and 5-keto-gluconate. With the API-ZYM system, This strain is found to have enzymatic activity to metabolize the following substrates: esterase (C4), leucine allyl amidase, valine allyl amidase, cysteine allyl amidase, acid phosphatase, naphthol-AS-BI-phosphohydrolase, α-galactosidase, β-galactosidase, α-glucosidase, β-glucosidase, and *N*-acetyl-β-glucosaminidase, but not metabolize alkaline phosphatase, esterase-lipase (C8), Lipase (C14), trypsin, α-chymotrypsin, β-glucuronidase, α-mannosidase, and α-frucosidase. The predominant cellular fatty acid is anteiso-$C_{15:0}$. The major menaquinone is MK-10. The major polar lipids are DPG, PI, AGPL, and GPL. The peptidoglycan type is A4β with L-Orn–D-Ser–D-Glu. The GC content of the type strain is 73.1 mol %.

The type strain is NTE-D12^T (= NBRC 115591^T = DSM 114595^T), isolated from an electrochemical enrichment of a culture derived from soil that had been passed through a 0.22 µm filter. The original soil was collected from Fukushima prefecture, Japan (37° 21′ N, 141° 01′ E).

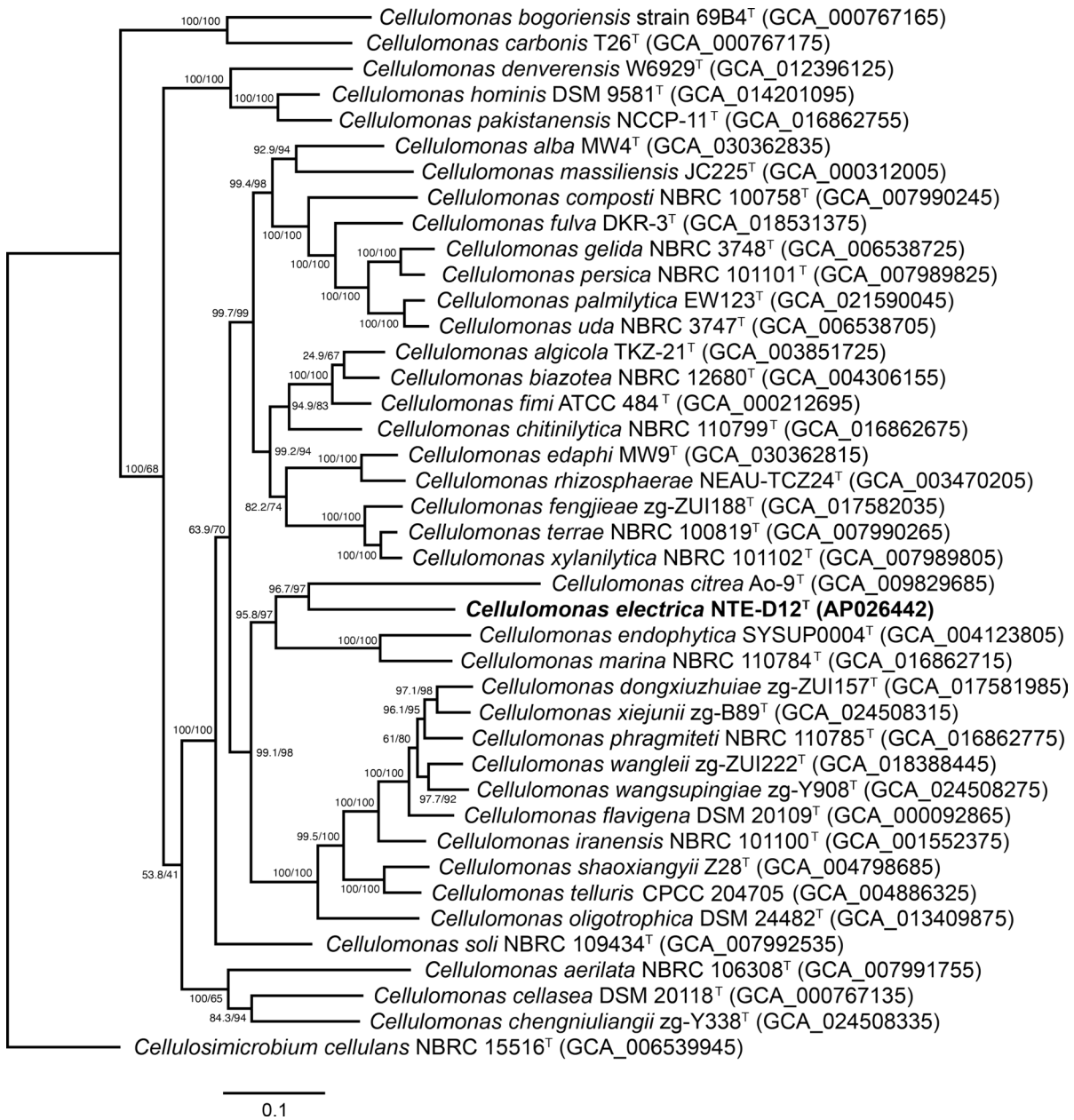

Fig. 2 Maximum-likelihood phylogenomic tree of strain NTE-D12^T and related *Cellulomonas* type strains. The tree was constructed using IQ-TREE2 v2.3.6 with the LG + F + G4 substitution model based on single-copy housekeeping genes identified and aligned with the GTDB-Tk v2.4.0 with the Bac120 gene marker set. Branch support values indicate ultrafast bootstrap (1,000 replicates) and SH-aLRT (1,000 tests). Nodes with ≥ 95% bootstrap and ≥ 80% SH-aLRT support were considered reliable (Minh et al. 2013). Bar, 0.1 nucleotide substitution position

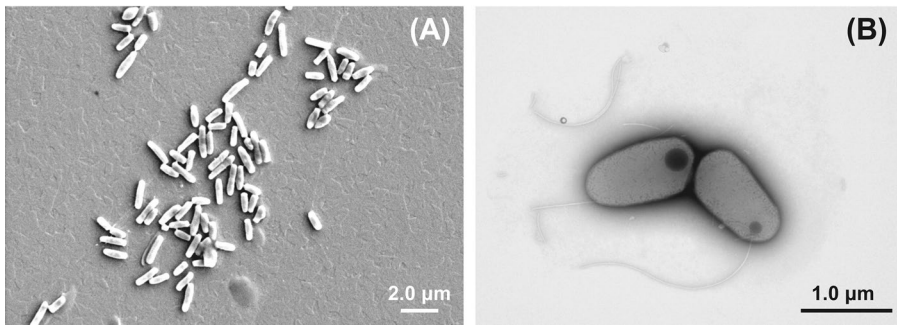

Fig. 3 Microscopic images of strain NTE-D12^T after incubation using R2A medium aerobically. **A** SEM images of the cells on the glass. **B** TEM image shows a flagellum from the cells

Acknowledgements The authors gratefully thank Dr. Satoshi Wakai, Dr. Shin-ichi Hirano, Dr. Yuma Dotsuta, Dr. Kyohei Otani, Dr. Toru Kitagaki, and Dr. Fumiyoshi Ueno for supporting the original sample collection.

Author contributions Conceptualization, S.I. and A.O.; Data Curation, S.I. and A.O.; Formal Analysis, S.I.; Funding Acquisition, S.I. and A.O.; Investigation, S.I.; Methodology, S.I.; Project Administration, A.O.; Resources, A.O.; Software, S.I.; Supervision, A.O.; Validation, S.I.; Visualization, S.I.; Writing—Original Draft, S.I.; Writing—Review & Editing, S.I. and A.O.

Funding This work was financially supported by a Grant-in-Aid for Research from the Japan Society for Promotion of Science (JSPS) KAKENHI (Grant No. 20H05590 and 22H02265), Grant-in-Aid for JSPS Fellows (Grant No. 24KJ0484) and PRIME from the Japan Agency for Medical Research and Development (Grant No. 19gm6010002h0004). This work was also supported by Japan Science and Technology Agency (JST), PRESTO (Grant No. JPMJPR19H1), the establishment of university fellowships towards the creation of science technology innovation (Grant No. JPMJSP2124) and by the JAEA Nuclear Energy S&T and Human Resource Development Project through concentrating wisdom (Grant No. PJA20P20333393). I.S. was supported by a grant from JST and JSPS.

Data availability The sequence data of Genbank/EMBL/DDBJ accession number AP026442 was used as a complete genome of strain NTE-D12^T. The 16S rRNA sequence data has been deposited to the DNA Data Bank of Japan (DDBJ) under accession number LC779660.

Declarations

Conflict of interest The authors declare no competing interests.

Ethical approval Not applicable.

References

Altschul SF, Gish W, Miller W, Myers EW, Lipman DJ (1990) Basic local alignment search tool. J Mol Biol 215:403–410

Auch AF, von Jan M, Klenk HP, Goker M (2010) Digital DNA-DNA hybridization for microbial species delineation by means of genome-to-genome sequence comparison. Stand Genomic Sci 2:117–134. https://doi.org/10.4056/sigs.531120

Bergey D, Harrison F, Breed R, Hammer B, Huntoon F (1923) Bergey's Manual of Determinative Bacteriology, 1st ed.

Bligh EG, Dyer WJ (1959) A rapid method of total lipid extraction and purification. Can J Physiol Pharmacol 37:911–917

Brosius J, Palmer ML, Kennedy PJ, Noller HF (1978) Complete nucleotide sequence of a 16S ribosomal RNA gene from Escherichia coli. Proc Natl Acad Sci 75:4801–4805

Capella-Gutierrez S, Silla-Martinez JM, Gabaldon T (2009) trimAl: a tool for automated alignment trimming in large-scale phylogenetic analyses. Bioinformatics 25:1972–1973. https://doi.org/10.1093/bioinformatics/btp348

Chklovski A, Parks DH, Woodcroft BJ, Tyson GW (2023) CheckM2: a rapid, scalable and accurate tool for assessing microbial genome quality using machine learning. Nat Methods 20:1203–1212. https://doi.org/10.1038/s41592-023-01940-w

Edgar RC (2004) MUSCLE: multiple sequence alignment with high accuracy and high throughput. Nucleic Acids Res 32:1792–1797. https://doi.org/10.1093/NAR/GKH340

Felsenstein J (1981) Evolutionary trees from DNA sequences: a maximum likelihood approach. J Mol Evol 17:368–376
Felsenstein J (1985) Confidence limits on phylogenies: an approach using the bootstrap. Evolution 39:783–791. https://doi.org/10.1111/J.1558-5646.1985.TB00420.X
Gerhardt P et al. (1981) Manual of methods for general bacteriology., Washington, DC
Goris J, Konstantinidis KT, Klappenbach JA, Coenye T, Vandamme P, Tiedje JM (2007) DNA-DNA hybridization values and their relationship to whole-genome sequence similarities. Int J Syst Evol Microbiol 57:81–91. https://doi.org/10.1099/ijs.0.64483-0
Hall T (1999) BioEdit: a user-friendly biological sequence alignment editor and analysis program for Windows 95/98/NT. Nucleic Acids Symp Ser 41:95–98
Hood MA, MacDonell M (1987) Distribution of ultramicrobacteria in a gulf coast estuary and induction of ultramicrobacteria. Microb Ecol 14:113–127
Ihara S, Wakai S, Maehara T, Okamoto A (2022) Electrochemical enrichment and isolation of electrogenic bacteria from 0.22 μm filtrate. Microorganisms. https://doi.org/10.3390/microorganisms10102051
Kang M-S et al (2007) Cellulomonas composti sp. nov., a cellulolytic bacterium isolated from cattle farm compost. Int J Syst Evol Microbiol 57:1256–1260
Khawdas W, Watanabe K, Karatani H, Aso Y, Tanaka T, Ohara H (2019) Direct electron transfer of *Cellulomonas fimi* and microbial fuel cells fueled by cellulose. J Biosci Bioeng 128:593–598. https://doi.org/10.1016/j.jbiosc.2019.05.001
Konstantinidis KT, Rosselló-Móra R, Amann R (2017) Uncultivated microbes in need of their own taxonomy. ISME J 11:2399–2406
Lee I, Ouk Kim Y, Park SC, Chun J (2016) OrthoANI: An improved algorithm and software for calculating average nucleotide identity. Int J Syst Evol Microbiol 66:1100–1103. https://doi.org/10.1099/ijsem.0.000760
Lee HJ, Kim SY, Whang KS (2020) *Cellulomonas citrea* sp. nov., isolated from paddy soil. Int J Syst Evol Microbiol 70:5304–5311. https://doi.org/10.1099/ijsem.0.004409
Li Y-Q et al (2020) Cellulomonas endophytica sp. nov., isolated from Gastrodia elata Blume. Int J Syst Evol Microbiol 70:3091–3095
Light SH et al (2018) A flavin-based extracellular electron transfer mechanism in diverse Gram-positive bacteria. Nature 562:140–144. https://doi.org/10.1038/s41586-018-0498-z
Lovley DR, Phillips EJ (1988) Novel mode of microbial energy metabolism: organic carbon oxidation coupled to dissimilatory reduction of iron or manganese. Appl Environ Microbiol 54:1472–1480
Minh BQ, Nguyen MAT, Von Haeseler A (2013) Ultrafast approximation for phylogenetic bootstrap. Mol Biol Evol 30:1188–1195
Minh BQ et al (2020) IQ-TREE 2: New Models and Efficient Methods for Phylogenetic Inference in the Genomic Era. Mol Biol Evol 37:1530–1534. https://doi.org/10.1093/molbev/msaa015
Minnikin DE, Patel PV, Alshamaony L, Goodfellow M (1977) Polar lipid composition in the classification of Nocardia and related bacteria. Int J Syst Evol Microbiol 27:104–117
Myers CR, Nealson KH (1988) Bacterial manganese reduction and growth with manganese oxide as the sole electron acceptor. Science 240:1319–1321
Naganuma T, Miyoshi T, Kimura H (2007) Phylotype diversity of deep-sea hydrothermal vent prokaryotes trapped by 0.2- and 0.1-μm-pore-size filters. Extremophiles 11:637–646. https://doi.org/10.1007/S00792-007-0070-5/TABLES/5
Nakai R et al (2013) Phylogeographic analysis of filterable bacteria with special reference to *Rhizobiales* strains that occur in cryospheric habitats. Antarct Sci 25:219–228. https://doi.org/10.1017/S0954102012000831
Naradasu D, Miran W, Sakamoto M, Okamoto A (2019) Isolation and characterization of human gut bacteria capable of extracellular electron transport by electrochemical techniques. Front Microbiol. https://doi.org/10.3389/fmicb.2018.03267
Naradasu D, Guionet A, Miran W, Okamoto A (2020) Microbial current production from *Streptococcus mutans* correlates with biofilm metabolic activity. Biosens Bioelectron 162:112236–112236. https://doi.org/10.1016/J.BIOS.2020.112236
Pankratova G, Hederstedt L, Gorton L (2019) Extracellular electron transfer features of Gram-positive bacteria. Anal Chim Acta 1076:32–47. https://doi.org/10.1016/J.ACA.2019.05.007
Qin Q-L et al (2014) A proposed genus boundary for the prokaryotes based on genomic insights. J Bacteriol 196:2210–2215
Rosselló-Mora R, Amann R (2001) The species concept for prokaryotes. FEMS Microbiol Rev 25:39–67
Saitou N, Nei M (1987) The neighbor-joining method: a new method for reconstructing phylogenetic trees. Mol Biol Evol 4:406–425. https://doi.org/10.1093/OXFORDJOURNALS.MOLBEV.A040454
Schumann P (2011) Peptidoglycan structure. Methods in microbiology. Elsevier, pp 101–129
Schumann P et al (2021) Reclassification of Haloactinobacterium glacieicola as Occultella glacieicola gen. nov., comb. nov., of Haloactinobacterium album as Ruania alba comb. nov, with an emended description of the genus Ruania, recognition that the genus names Haloactinobacterium and Ruania are heterotypic synonyms and description of Occultella aeris sp. nov., a halotolerant isolate from surface soil sampled at an ancient copper smelter. Int J Syst Evol Microbiol. https://doi.org/10.1099/ijsem.0.004769
Shi L et al (2016) Extracellular electron transfer mechanisms between microorganisms and minerals. Nat Rev Microbiol 14:651–662. https://doi.org/10.1038/nrmicro.2016.93
Sun X, Li J, Du J, Xiao H, Ni J (2018) *Cellulomonas macrotermitis* sp. nov., a chitinolytic and cellulolytic bacterium isolated from the hindgut of a fungus-growing termite. Antonie Van Leeuwenhoek 111:471–478. https://doi.org/10.1007/S10482-017-0968-6/FIGURES/1
Takahashi K, Nei M (2000) Efficiencies of fast algorithms of phylogenetic inference under the criteria of maximum parsimony, minimum evolution, and maximum likelihood when a large number of sequences are used. Mol Biol Evol 17:1251–1258
Tamaoka J, Katayama-Fujimura Y, Kuraishi H (1983) Analysis of bacterial menaquinone mixtures by high performance liquid chromatography. J Appl Bacteriol 54:31–36. https://doi.org/10.1111/j.1365-2672.1983.tb01297.x

Tamura K, Stecher G, Kumar S (2021) MEGA11: molecular evolutionary genetics analysis version 11. Mol Biol Evol 38:3022–3027

Wrighton KC et al (2011) Evidence for direct electron transfer by a gram-positive bacterium isolated from a microbial fuel cell. Appl Environ Microbiol 77:7633–7639. https://doi.org/10.1128/AEM.05365-11

Yamamura H et al (2019) *Cellulomonas algicola* sp. nov., an actinobacterium isolated from a freshwater alga. Int J Syst Evol Microbiol 69:2723–2728. https://doi.org/10.1099/ijsem.0.003549

Yassin AF, Haggenei B, Budzikiewicz H, Schaal KP (1993) Fatty acid and polar lipid composition of the genus amycolatopsis: application of fast atom bombardment-mass spectrometry to structure analysis of underivatized phospholipids. Int J Syst Evol Microbiol 43:414–420

Zhang L et al (2013) *Cellulomonas marina* sp. nov., isolated from deep-sea water. Int J Syst Evol Microbiol 63:3014–3018. https://doi.org/10.1099/ijs.0.048876-0